Slowing the translocation of double-stranded DNA using a nanopore smaller than the double helix

Utkur Mirsaidov[1]**, Jeffrey Comer**[1,2]**, Valentin Dimitrov**[1]**,
Aleksei Aksimentiev**[1,2] **and Gregory Timp**[1,3]

[1] Beckman Institute, University of Illinois, Urbana, IL 61801, USA
[2] Department of Physics, University of Illinois, Urbana, IL 61801, USA
[3] Stinson-Remick Hall, University of Notre Dame, Notre Dame, IN 46556, USA

Abstract
It is now possible to slow and trap a single molecule of double-stranded DNA (dsDNA), by
stretching it using a nanopore, smaller in diameter than the double helix, in a solid-state
membrane. By applying an electric force larger than the threshold for stretching, dsDNA can be
impelled through the pore. Once a current blockade associated with a translocating molecule is
detected, the electric field in the pore is switched in an interval less than the translocation time
to a value below the threshold for stretching. According to molecular dynamics (MD)
simulations, this leaves the dsDNA stretched in the pore constriction with the base-pairs tilted,
while the B-form canonical structure is preserved outside the pore. In this configuration, the
translocation velocity is substantially reduced from 1 bp/10 ns to ~1 bp/2 ms in the extreme,
potentially facilitating high fidelity reads for sequencing, precise sorting, and high resolution
(force) spectroscopy.

S Online supplementary data available from stacks.iop.org/Nano/21/395501/mmedia

1. Introduction

Atoms can be slowed and subsequently trapped for precise characterization and manipulation using optical intensity gradients and the corresponding light pressure forces [1]. Molecules, on the other hand, have a more complex energy-level structure. Lacking a closed, two-level energy system, molecular population dynamics are more difficult to control, which generally precludes manipulation by optical trapping directly. Instead, to manipulate them researchers have resorted to electrostatic fields defined by microfabrication on a chip [2, 3]. Thus, just like for an optical trap, strong field gradients in this case controlled by the lithography are used to slow and trap molecules.

We are motivated to slow and trap a single DNA molecule for sequencing applications [4] and for measurements of the electromechanics of DNA on the scale of a protein binding site (3–10 nm) [5, 6]—providing information that is vital for understanding how gene transcription, replication and silencing work. Applications like these, along with the structure of DNA, impose especially stringent specifications on

the trap that can only be addressed with nanofabrication. B-form double-stranded DNA (dsDNA) is a stiff, highly charged polymer with a twisting, propeller-like, helical structure ~2 nm in diameter with an axial rise of 0.34 nm/base-pair [7]. By scrupulous design, the electric potential gradient in a nanometer-diameter pore can have comparable dimensions to dsDNA. Moreover, the force associated with the electric potential can be used to impel a dsDNA molecule to translocate through a pore, even if the diameter is smaller than the double helix.

Prior work has established that there is a voltage threshold for permeation of dsDNA through $d < 3$ nm pores, corresponding to the force required to stretch the leading nucleotides in the pore [8, 9]. For a bi-conical pore geometry, the leading edge of the dsDNA penetrates into the membrane to a constriction of about $d \sim 2.5$ nm. If the differential force acting on the leading nucleotides is insufficient to stretch the helix, the translocation stalls there. It stalls because, while dsDNA has a helical structure ~2 nm in diameter, the solvated structure is about 2.6–2.9 nm in diameter (according to neutron scattering) [7]. As the bias increases and the differential force on the leading nucleotides exceeds that required to stretch

0957-4484/10/395501+10$30.00

1

dsDNA, the molecule is pulled towards the center of and eventually through the membrane. The confinement in pores with diameters 1.6 nm $< d <$ 2.5 nm causes the base-pairs to tilt [6, 10].

Following preliminary reports described elsewhere [11, 12], we have developed a method that uses a time-varying electric field and the stretching transition to slow and trap a single molecule of dsDNA in a nanopore in a solid-state membrane. It is now possible to trap a single dsDNA molecule in a nanopore <3 nm in diameter for up to 2 min by first applying a voltage larger than this threshold and forcing the molecule to translocate through the pore. If the electric field is then rapidly switched to a value below threshold during the translocation, a single λ-DNA molecule becomes trapped for seconds to minutes in the pore, whereas the λ-DNA translocates in <1 ms if the field is maintained above threshold. Molecular dynamics (MD) simulations of these experiments reveal that, when trapped, the dsDNA is stretched in the pore constriction in a specific tilted orientation, depending on the orientation of the leading nucleotides, while the B-form canonical structure is preserved outside the pore. Moreover, commensurate with the bandwidth of the nanopore, if the duration of the trap is extremely long, we observe in the ion current what may be signatures of the base-pairs translocating through the pore.

2. Experimental and simulation details

The fabrication of a nanopore in silicon nitride membranes 50 μm $\times$ 50 μm is described elsewhere [13]. Nominally, the thickness of the membrane is 30 nm. To reduce the thickness to about 15 nm, the membrane is uniformly etched in 20:1 H_2O:49% HF for 30–40 min at room temperature. After a 10 s O_2 plasma clean, the thickness of the exposed nitride membrane is measured *in situ* using electron energy loss spectroscopy, and then a nanometer-size pore is sputtered in it using a tightly focused (1.3 nm spot-size) 9° α (cone angle), high energy (200 kV) electron beam emanating from a JEOL 2010-F transmission electron microscope (TEM) operating in convergent beam diffraction mode, biased at 170 μA emission current, using a 150 mm condenser aperture. The sputtering time is typically about ∼30 s. Using TEM images taken at different tilt angles, we model the pore geometry as two intersecting cones (bi-conical) each with >20° cone angle [13].

After sputtering, a membrane with a pore in it is subjected to a standard clean in (7:3) H_2SO_4:H_2O_2 for 3 min. Subsequently, the membrane chip is mounted in a two-chamber acrylic holder. Silicone O-rings are used to seal the chip into the holder between the two chambers, leaving the nanopore as the only connection between the two chambers. The *cis* chamber has a volume of 100 μl; the *trans* chamber has a volume of approximately 13 ml. Voltage is applied and the DC, AC, current response and noise characteristics of the nanopore are measured in 100 mM KCl solution at 23 $\pm$ 1 °C using Ag/AgCl electrodes (Warner) in each chamber. The electrolytic current is measured using an Axopatch 200B.

Switching the electric field at high-speed demands a nanopore with a high frequency response [14]. So, we measured the current response of the pore and used it to create a comprehensive, small signal model derived from the nanostructure. The frequency response of nanopores was measured using a Signal Recovery 7280 lock-in amplifier. A small AC voltage signal (50 mV rms amplitude) at various frequencies is applied to the *cis* chamber, and the in-phase and out-of-phase components of the membrane current or voltage are measured by a phase-sensitive lock-in technique. In the supplement, figure S1(a) (available at stacks.iop.org/Nano/21/395501/mmedia) shows the current frequency response of a 15 nm thick membrane with a 2.5 nm diameter pore in it. A detailed model that accurately accounts for the frequency response of the nanopore, which is rooted in the physical structure and reflects in a limited way the distributed nature of the electrical parameters is shown in figure S1(b) (available at stacks.iop.org/Nano/21/395501/mmedia).

From this analysis we deduce that the frequency response of these membranes cannot be accurately represented by the single capacitor model as suggested by Smeets *et al* [15], but rather consists of a parallel combination of three high pass filters along with the pore resistance. Relying on the model, it is also possible to describe the relationship between the AC pore current and the AC voltage responses across the membrane. In the supplement, we show measurements and simulations of the voltage transient associated with an input voltage step from 1 to 0 V applied across the Ag/AgCl electrodes spanning the membrane. The voltage decays with a time constant of about $\tau = 210$ ns. According to the model, the membrane voltage tracks the input transient, but with a slower time constant: i.e. $\tau = 460$ ns associated with the electrolyte resistance $R_{el} = 4.6$ kΩ and an effective capacitance $C_{eff} = 118$ pF, which is derived from the membrane window capacitance, $C_{win} = 11.9$ pF in parallel with the series combination of the Si depletion capacitances $C_{dt} = 127$ pF and $C_{db} = 666$ pF.

MD simulations were performed following protocols described elsewhere [8–10, 16, 17]. These simulations used the program NAMD2, a 1.0 fs time step, periodic boundary conditions, and particle mesh Ewald electrostatics (grid spacing < 0.15 nm). In the simulations employing the CHARMM27 and BKS force fields, the van der Waals energies were computed using smooth 1.0–1.2 nm and 0.54–0.55 nm cutoffs, respectively.

Two nanopore systems with different cross sections were created. The first nanopore system used a modified version of the silica model described in Cruz-Chu *et al* [18]. To produce the first nanopore system, a block of crystalline silica containing 13 000 silicon and 26 000 oxygen atoms was melted in an MD simulation using the modified BKS force field [19, 20]; an external potential expelled atoms from the region that would become the pore [21]. The silica was annealed for 50 ps at 7000 K, 50 ps at 500 K, 50 ps at 2000 K, and 50 ps at 300 K; the temperature was controlled using a Langevin thermostat with a damping coefficient of 5 ps^{-1}. The resulting pore had a shape of two intersecting cones each making a 20° angle with the pore axis. The minimum cross-section of the pore was a 2.6 nm $\times$ 2.1 nm ellipse located at the center of the 10 nm thick membrane.

In all further simulations, the atoms of the membrane were restrained to their positions at the end of the annealing process. Harmonic restraints of 13.9 nN nm^{-1} were used to implement the restraints; additional harmonic bonds of 695 pN nm^{-1} were applied between silicon and oxygen atoms within 0.22 nm of each other. These bond and restraint force constants gave the membrane a dielectric constant of ∼5. The charges of the silicon and oxygen atoms and their Lennard-Jones parameters were taken from Cruz-Chu *et al* [18]. A 60-base-pair fragment of B-form dsDNA was inserted halfway through the pore. The 3′ and 5′ ends of the DNA fragment were covalently linked across the periodic boundaries, making the molecule effectively infinite.

The second nanopore system used a silicon nitride model described previously [9, 10]. A β-Si$_3$N$_4$ crystal was replicated to produce a hexagonal prism of crystalline material with hexagonal side lengths of 4.56 nm and a thickness of 10.5 nm. A double cone pore having a circular cross-section with a minimum diameter of 2.0 nm was cut into the hexagonal prism by removal of atoms [10]. The cones made an angle of 10° with the pore axis. The charges of the silicon and nitrogen atoms and their Lennard-Jones parameters were taken from Wendel and Goddard [22]. Bonds were added between adjacent atoms with the bond constants of 3470 pN nm^{-1} [10]. The atoms were constrained to their initial positions by restraints of 695 pN nm^{-1} to obtain a dielectric constant of 7.5. To obtain a realistic conformation of dsDNA confined in the 2.0 nm pore, a 58-base-pair fragment of B-form dsDNA was simulated in solution under the influence of a phantom pore [9] with the minimum radius being reduced from 2.8 to 2.0 nm over 6 ns. The ends of the molecule were not covalently linked as above.

Both DNA–nanopore structures were solvated with 100 mM KCl electrolyte, forming systems of about 120 000 atoms. Each system underwent 2000 steps of energy minimization and a 300 ps equilibration with the pressure maintained at 1 atm and the temperature maintained at 295 K. To ensure that the DNA conformation in the 2.0 nm silicon nitride pore was fully relaxed, the system was further equilibrated at fixed volume for 7 ns. Both nanopore systems were then simulated with various external electrostatic biases applied. During these simulations, the volume of the system was fixed and the temperature was maintained at 295 K by applying the Langevin thermostat to only atoms of the membrane with a damping coefficient of 1 ps^{-1}.

3. Results and discussion

A TEM image of a nanopore with a 2.5 nm×2.0±0.2 nm cross-section—smaller than the DNA double helix—in a membrane 15.0 ± 2.2 nm thick is shown in figure 1(a). When λ-DNA is injected into the electrolyte at the negative (*cis*) electrode and 800 mV applied across the membrane, current transients like those shown in figure 1(b) are observed. The transients occur randomly as a function of time, but the inter-arrival time decreases with increasing concentration of DNA on the *cis* side of the bi-cell. There are a variety of current transients, some of which are illustrated in figure 1(c). We speculate that the disparity in shape and duration of the current transients reflects

the molecular configuration in the neighborhood of the pore and the time required to disentangle the DNA in solution into the single file of base-pairs required to permeate the pore [10]. The distribution of transients can be represented by a blockade with a peak value at $\Delta I/I_0 = 0.62 \pm 0.11$ of the open pore current as shown in figure 1(d). A blockade is caused by the reduction of the electrolytic current through the pore due to the translocation of DNA. In support of this interpretation, MD estimates also indicate a $\Delta I/I_0 = 0.71 \pm 0.07$ blockade through a 2.0 nm diameter pore in 100 mM KCl.

Figure 1(b) illustrates threshold behavior, showing a dearth of transients found in a current trace measured at 200 mV compared to an 800 mV trace. Figure 1(e) summarizes the voltage dependence of the frequency of blockade events over the range from 100 mV to 1 V. Generally, we observe an abrupt rise in the number of blockades over a range of ∼200 mV near a threshold that is sensitive to the pore diameter. If we assume each blockade corresponds to dsDNA permeating the pore, then the permeation rate can be described by a transition-state relation of the Kramers type: $R = R_0 V/(1 + \exp[q^*(U - V)/kT])$, where R_0 is a frequency factor, q^*U is the effective barrier height, q^*V is the reduction in the energy barrier due to the applied potential, and kT is the thermal energy [23]. Using this relation, the data were fitted and the results were overlaid on the scatter plot in figure 1(e). We find a threshold of $U = 0.46 \pm 0.02$ V with $q^* = 0.8 \pm 0.2e$, which presumably corresponds to the force required to stretch the leading nucleotides in the pore—below this voltage DNA is not supposed to permeate the membrane.

The dependence of the blockade duration on the membrane voltage offers more support to the interpretation of the blockade current as a translocation across the membrane. Figure 1(f) shows the frequency of current transients associated with λ-DNA as a function of duration with the voltage as a parameter. If the blockade duration corresponds with the interval that DNA blocks the pore, then the average transient width t_D signifies the time required for 48.502 kbp λ-DNA to translocate through the pore. We find that $t_D = 0.16 \pm 0.01$ ms, 0.53 ± 0.06 ms, 1.1 ± 0.1 ms, 0.82 ± 0.07 ms and 2.49 ± 0.25 ms for voltages of 1.0 V, 800 mV, 700 mV, 600 mV and 500 mV, respectively. The corresponding translocation velocity is 1 bp/3.3 ns at 1 V and 1 bp/11 ns at 800 mV to 1 bp/50 ns at 500 mV, which is consistent with MD (see figure 5). The inset to figure 1(f) shows a plot of the voltage dependence of the reciprocal of the average transient width, i.e. $1/t_D$, measured above threshold. $1/t_D$ vanishes near the threshold value. The line in the inset is a least-squares fit to the data. It has a slope of 11 V^{-1} s^{-1} with a voltage-intercept of 0.53 V that is comparable to the threshold voltage inferred from figure 1(e).

These observations are in sharp contrast with prior work on larger diameter pores, and measurements that we performed on a pore with cross-section 3.6 nm × 3.2 ± 0.2 nm in a 31.5 ± 2.0 nm thick nitride membrane. In the supplement, we show that, if there is a threshold for permeating a 3.6 nm × 3.2 nm pore, it is very low ($U < 17 \pm 11$ mV) and the transient widths $t_D = 0.031 \pm 0.007$ ms, 0.032 ± 0.007 ms, 0.068 ± 0.003 ms, and 0.403 ± 0.260 ms measured for transmembrane
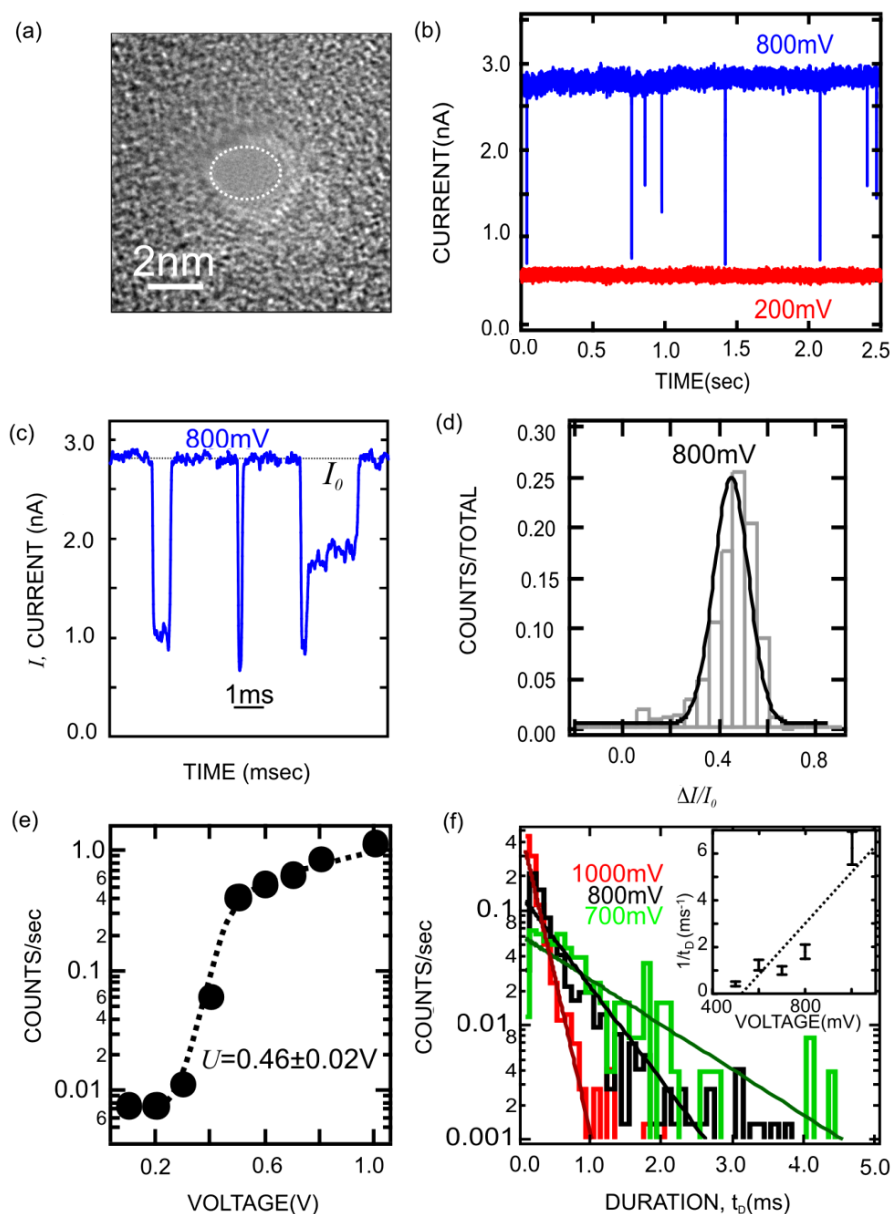
Figure 1. (a) A TEM image of a 2.5 nm × 2.0 nm cross-section pore in a silicon nitride membrane 15.0 nm thick. (b) Electrolytic current measured in 100 mM KCl at 800 mV (blue) and 200 mV (red) through the pore shown in (a) as a function of time. The frequency of blockades decreases dramatically with voltage; at 0.2 V no transients are observed. (c) Three examples of current blockades observed in the pore shown in (a) at $V = 800$ mV under the same conditions as (b). These blockades are all associated with λ-DNA translocating through the pore. (d) The frequency of blockades observed at 800 mV with a particular change in current normalized to the open pore current in the same pore. (e) The frequency of blockades observed with the 2.5 nm pore as a function of membrane voltage, illustrating the frequency drop as voltage decreases below 0.5 V. The dotted line represents a fit to the data. (f) Distributions illustrating the frequency as a function of the duration of a current blockade, t_D, above threshold at 1.0 V (red), 800 mV (black), and 700 mV (green). The distribution depends sensitively on the voltage. Inset: the reciprocal of the duration, t_D^{-1}, as a function of the applied voltage.

voltages of 600 mV, 400 mV, 200 mV and 100 mV respectively, correspond to translocation velocities ranging from 1 bp/0.6 ns to 1 bp/8.3 ns, which exceed the velocities found using smaller pores, and yet are consistent with prior estimates [24, 25].

The voltage-intercept for $1/t_D$ near the threshold suggests that dsDNA can be trapped in a nanopore that is smaller in diameter than the double helix. To test this hypothesis first we forced dsDNA into a 2.5 nm pore and then, when a blockade in the current was detected, reduced the transmembrane bias while the DNA was still in the pore. Once the dsDNA is in

the pore, if the bias is reduced below the stretching threshold, the pore is supposed to act as a trap resisting the motion of the molecule.

Figures 2(a) and (b) show data demonstrating that it is possible to slow or weakly trap a single λ-DNA molecule in the pore by switching the electric field. First, a transmembrane bias of 800 mV, which is above threshold according to figure 1(e), is applied. Once the onset of a blockade like that shown in the inset to figure 2(a) is detected by the differentiator, a programmed delay of 200 μs is introduced before a latch
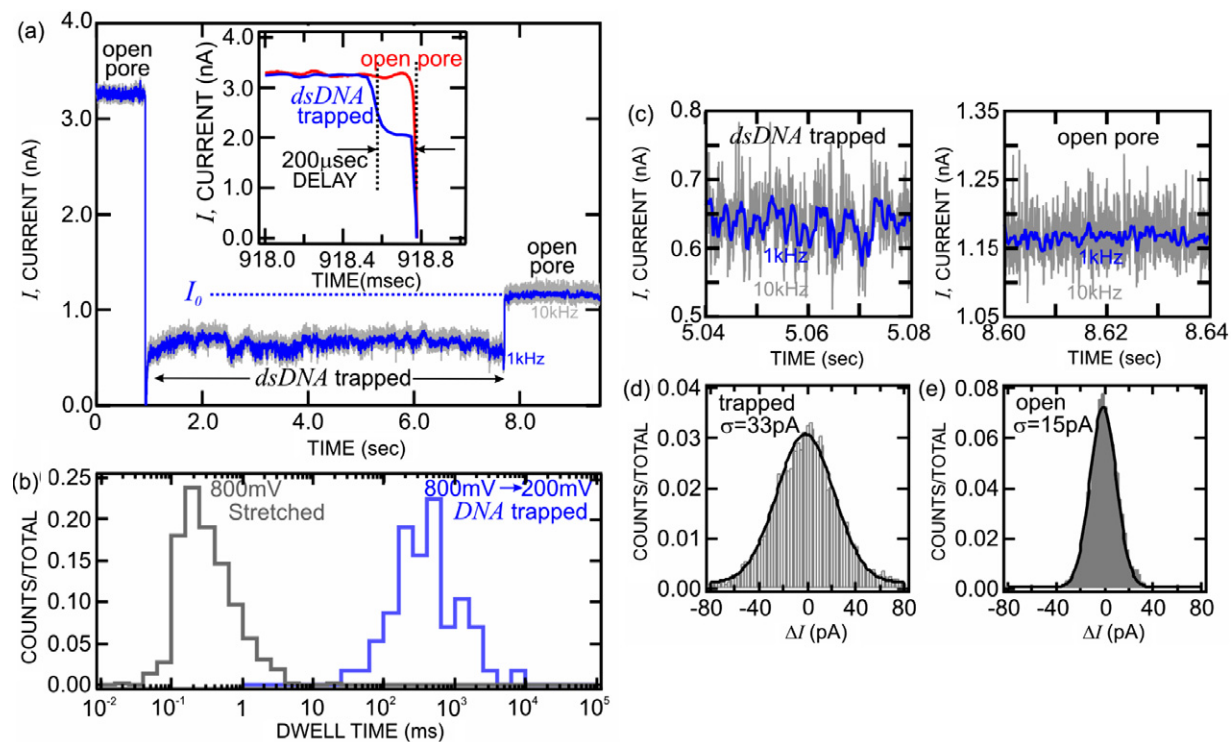
Figure 2. Trapping a λ-DNA molecule in a nanopore. (a) Upon detection of a current blockade indicating that dsDNA is translocating through the 2.5 nm pore (shown in figure 1(a)), the voltage across the pore is switched from 800 mV (above the stretching threshold) to 200 mV (below threshold). As a result, the duration of the current transient (blue) increases from ~200 μs to about 6.79 s. The transient observed at 7.709 s is supposed to indicate a single λ-DNA molecule exiting the pore. The gray trace represents data taken with a bandwidth of 10 kHz; the blue trace is the same data with a 1 kHz (8-pole Bessel) filter. Inset: detail showing the onset of a current transient and the 200 μs built-in delay executed before triggering the voltage pulse. (b) Histograms showing the distribution of dwell times observed at 800 mV (gray) and the distribution of elapsed time spanning the instant when a blockade event triggers the voltage switch from 800 to 200 mV to the return of the current to the open pore value seconds later (blue). The translocation time increases 1500×. (c) A magnified view of the pore current observed during (left) and after (right) the blockade showing the change in the magnitude of the current fluctuations. Histograms are shown quantifying the fluctuations in the current distribution of the normalized current during the blockade (d) and for the open pore (e) at 200 mV. The blockade current and open pore current fluctuations can be fitted with Gaussians that have widths of $\sigma = 33.6$ pA and $\sigma = 15.3$ pA respectively.

switches the voltage from 800 to 200 mV—a value well below the threshold. All the while, the pore current is monitored. In the supplement we show that the transmembrane voltage tracks the voltage applied to the Ag/AgCl electrodes, but with a longer time constant (<500 ns). Eventually, the blockade ends and the current returns to the open pore value, I_0, but not before we observe a sharp transient like that shown near $t = 7.709$ s in figure 2(a).

We supposed that transients like these are indicative of the λ-DNA molecule exiting the pore after 6.8 s. So, we reasoned that the current blockade observed during the time interval from $t = 0.918$ to 7.709 s must be evidence of a weakly trapped λ-DNA molecule in the pore. We do not observe a current blockade at 200 mV if there is no onset of a blockade at 800 mV. Moreover, as shown in the supplement, a larger (3.6 nm × 3.2 nm) pore at a constant bias of 200 mV shows a distribution of blockade durations that peaks near 200 μs but does not exceed 1 ms, making the long (6.8 s) duration shown in figure 2(a) extraordinary. If the molecule is weakly trapped in the pore, then the average translocation velocity must have slowed substantially to a value of about (48.5 kbp–200 μs×1 bp/11 ns)/6.8 s = 1 bp/224 μs, which is

about 20 000× slower than the velocity estimate for t_D obtained at 800 mV.

After repeating this type of measurement hundreds of times on the same pore, a comparison between the distribution of the duration of blockades observed with a transmembrane bias of 800 mV, and the time that expires between the triggered voltage switch from 800 to 200 mV and the return of the current to the open pore value reveals the dichotomy illustrated in figure 2(b). While the peak in the distribution obtained at a constant bias of 800 mV occurs near $t_D = 200$ μs, the peak of the distribution found when the voltage is switched from 800 to 200 mV occurs near $t_D \sim 500$–600 ms. This suggests that the translocation velocity at the peak must have slowed substantially to a value of about (48.5 kbp–200 μs × 1 bp/11 ns)/500 ms = 1 bp/17 μs, which is about 1500× slower than the velocity obtained at 800 mV. In comparison, we do not observe blockades >4 ms at constant bias of 800 mV. Comparing the distribution of the normalized blockade current $\Delta I/I_0$ obtained at a constant bias of 800 mV with the blockades measured after switching the voltage from 800 to 200 mV, we find that they overlap within the error. The mean blockade signal fit to a Gaussian is $\Delta I/I_0 = 0.62 \pm 0.11$ at
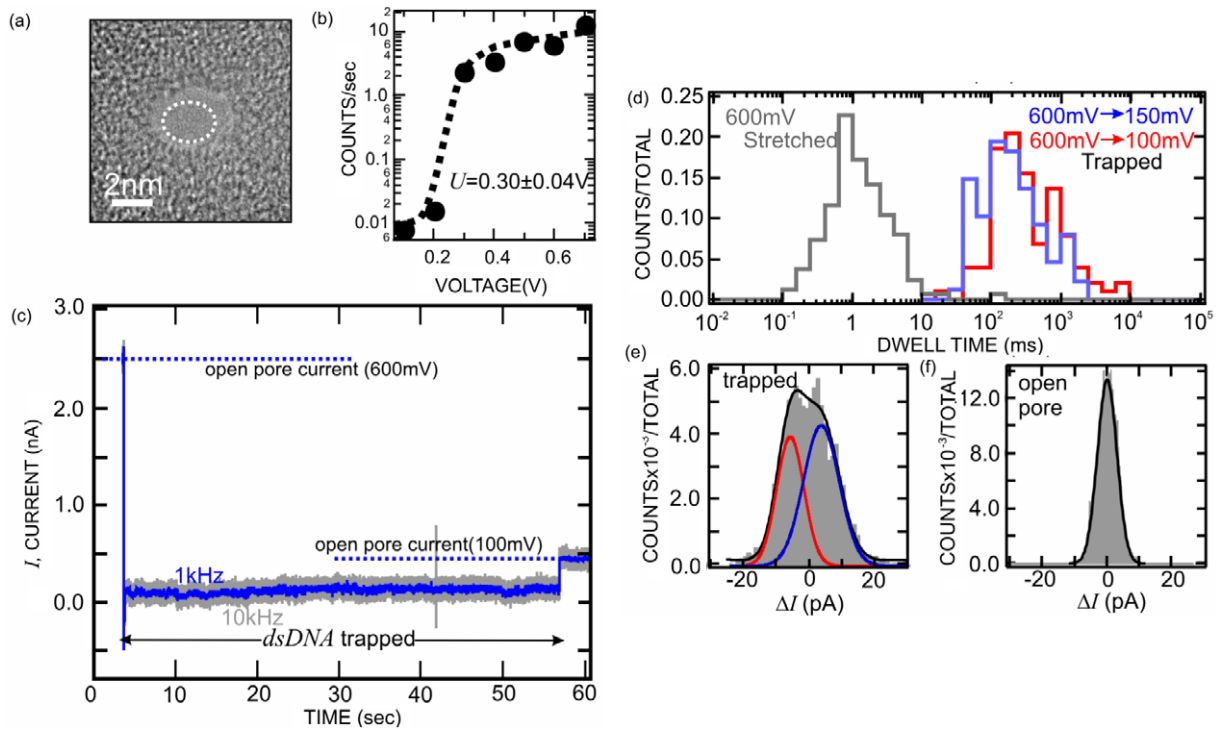
Figure 3. Trapping a λ-DNA molecule in a nanopore. (a) A TEM micrograph of a 2.6 nm × 2.0 nm cross-section pore in a silicon nitride membrane 15 nm thick. (b) The frequency of blockades observed with this pore as a function of membrane voltage illustrating the frequency drop as voltage decreases below 0.3 V. The dotted line represents a fit to the data. (c) Triggered by the onset of a current blockade indicating that dsDNA is translocating through the pore of (a), the voltage is switched from 600 mV (above the stretching threshold) to 100 mV (below threshold). As a result the molecule is trapped in the pore till $t = 58.8$ s. (d) Histograms showing the distribution of dwell times observed at 600 mV (gray) and the distribution of elapsed time spanning the instant when a blockade event triggers the voltage switch from 600 to 150 mV (blue) or 100 mV (red) to the return of the current to the open pore value seconds later. The peak in the distribution of current blockade durations (blue) increases from about 900 μs to about 200 ms, increasing 200×. (e), (f) Histograms showing the distribution of the current during the blockade in the interval 14–14.5 s, when λ-DNA is trapped (e), and the open pore for $t > 58.8$ s (f). The distribution for the trapped molecule must be fitted to at least two Gaussians: one (solid blue) offset from the median ($\Delta I = 0$) by $\Delta I = +2.86$ pA with a width of $\sigma = 7.8$ pA; and another (solid red line) offset by -6.51 pA with a width of $\sigma = 5.9$ pA. The black line represents the sum. In contrast, the data in (f) representing the open pore can be fitted by a single Gaussian with a width $\sigma = 4.26$ pA.

800 mV constant bias and 0.46±0.07 when the bias is switched from 800 to 200 mV.

The fluctuations illustrated in figures 2(c) and (d) support the hypothesis that the pore current is blockaded by λ-DNA. We observed that for $t < 7.709$ s the amplitude of the current fluctuations increases relative to the open pore value found for $t > 7.709$ s. Figure 2(c) differentiates the current fluctuations during the blockade from the open pore current. Focusing on the data filtered with a low-pass (8-pole Bessel) 1 kHz filter, the width of the histogram shown in figure 2(d) taken from the blockaded current is $\sigma = 33$ pA ($0.28I_0$) with $\chi^2 = 0.52$, while the open pore histogram measured over the same 0.5 s interval is only $\sigma = 15.3$ pA ($0.13I_0$) wide with $\chi^2 = 0.43$, indicating a signal beyond the noise for $t < 7.709$ that is due to base-pairs translocating through the pore. To corroborate this assertion, we and others [14, 26] have measured the low frequency current noise spectral density associated with a pore in a membrane in the absence of DNA. We have determined that the noise spectrum scales with the pore resistance according to: $S_{1/f} = I^2 A / f^\beta \propto I^2 R_p^n / f^\beta$, where I is the current through the device, f is the frequency, $\beta \approx 1$ is an exponent and R_p is the pore resistance with $n =$

1.06 ± 0.15. Accounting for the blockade of $\Delta I / I_0 = 0.5$ and the change in pore resistance, the current noise should decrease overall from the open pore value, yet we observe an increase by 2× instead. Thus, the large fluctuating current is due to the trapped dsDNA.

We have made similar findings on six pores with similar geometries. Figure 3 summarizes the results obtained on a 2.6 nm × 2.0 ± 0.2 nm pore. The threshold voltage for this pore derived from the fit to the data shown in figure 3(b) is estimated to be about $U = 0.30 \pm 0.04$ V (with $q^* = 1.1 \pm 0.2$). Figure 3(c) shows an extraordinary event obtained from this pore, which represents a λ-DNA molecule trapped by first applying a bias of 600 mV (above threshold) across the membrane and then, once the onset of a blockade is detected, switching the voltage to 100 mV (below threshold). Eventually, the current returns to the open pore value, near $t = 58.8$ s in figure 3(c). We assume that the transient at $t = 58.8$ s is indicative of the molecule exiting the pore after 56 s, corresponding to a translocation velocity of >1 bp/1.8 ms—about 97 000× slower than the peak value obtained at a constant bias of 600 mV.

For this pore, we also measured the blockade duration distribution at a constant bias of 600 mV and when the voltage

is switched from 600 to 150 mV and from 600 to 100 mV, 200 μs after detecting the onset of a blockade. Similar to the data presented in figure 2, we observed that the duration of the blockade is extended from an average of 900 μs to 200 ms— the velocity is $\sim$200$\times$ slower as illustrated by figure 3(d). In this case, the distribution of the normalized blockade current $\Delta I/I_0$ with a constant bias of 600 mV and the blockades measured after switching the voltage from 600 to 150 mV or 100 mV closely resemble each other—the former peaks at $\Delta I/I_0 = 0.62 \pm 0.11$, while the latter peak near $\Delta I/I_0 = 0.62 \pm 0.15$ and $\Delta I/I_0 = 0.59 \pm 0.15$ respectively. The apparent translocation velocity depends on the voltage applied after switching: i.e. the distribution found when we switch from 600 to 150 mV (100 mV) has a peak duration near 150 ms (200 ms) respectively.

Trapping a DNA molecule should facilitate the high fidelity reads required for sequencing it. With the molecule trapped (i.e. for $t < 58.8$ s in figure 3(c)), we filtered the current data using a 10–600 Hz bandpass filter and formed histograms of the current fluctuations using 0.5 s windows. Each window in the trapped data ($t < 58.8$ s) shows a histogram similar to that shown in figure 3(e), which can be represented by the superposition of two Gaussian distributions: one (solid blue) offset from the median ($\Delta I = 0$) by $\Delta I = +2.86$ pA with a width of $\sigma = 7.8$ pA; and another (solid red) offset by $\Delta I = -6.51$ pA with a width of $\sigma = 5.9$ pA. The goodness of fit, measured by the reduced chi-squared statistic, improves from $\chi^2 = 5.04$ for a single Gaussian fit to $\chi^2 = 0.71$ for two Gaussians, indicating that two Gaussians represent a superior model. This is in contrast to the data shown in figure 3(f), which represent the open pore current fitted by a single Gaussian with a width $\sigma = 4.26$ pA with $\chi^2 = 0.67$ measured at the same voltage.

We tentatively attribute the separate peaks in figure 3(e) at $\Delta I = +2.86$ pA and $\Delta I = -6.51$ pA to partially resolved signals associated with C–G/G–C and A–T/T–A base-pairs, respectively. This identification is supported by the observation that λ-DNA has a nearly uniform distribution of base-pairs T–A, A–T, C–G, G–C. Thus, the currents corresponding to each type of base-pair should translate to approximately equal, distinct distributions in the blockade current convolved with the electrical noise. The difference between C–G and A–T base-pairs can be resolved in this case because of the correspondingly longer ($\sim$2 ms) time each base-pair spends in the constriction compared with the (220 μs) peak dwell time for the molecule in pore of figure 2(a). However, apparently the signal-to-noise ratio is inadequate for discriminating C–G from G–C or A–T from T–A, despite the slowing. This assertion is also corroborated by even longer duration measurements of blockade currents associated with streptavidin bound, 100 bp long, C–G and A–T biotinylated duplexes trapped by the electric field in a pore in a configuration described elsewhere [27].

While a smaller diameter increases the signal (i.e. blockade current), there is a concomitant increase in noise as well. Figure 4 summarizes the results obtained on the smaller pore, 2.2 nm $\times$ 1.8 $\pm$ 0.2 nm in cross-section, shown in (a). The threshold estimated from the voltage dependence of the
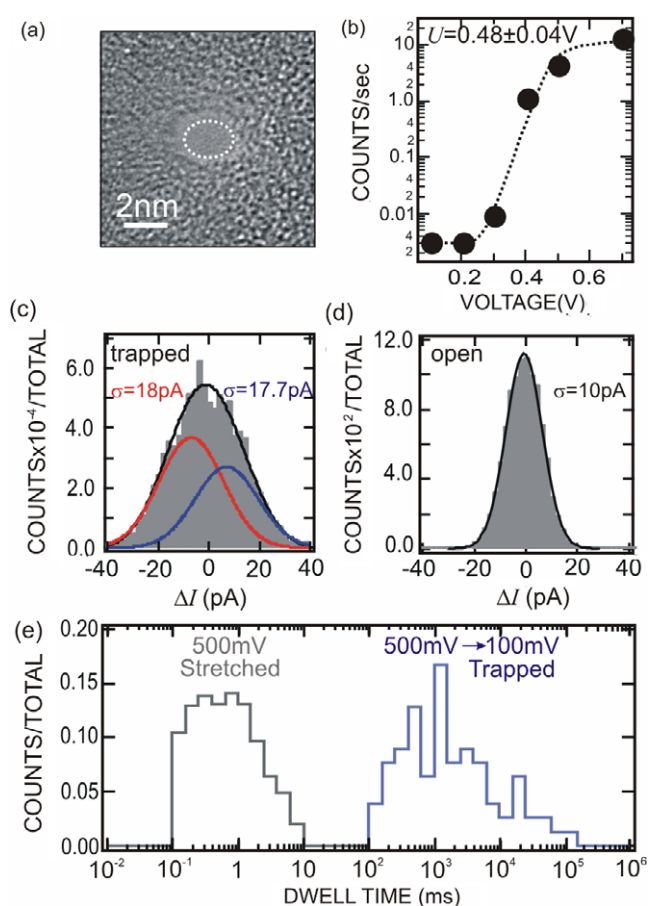

Figure 4. Trapping a λ-DNA molecule in a nanopore. (a) A TEM micrograph of a 2.2 nm $\times$ 1.8 nm cross-section pore in a silicon nitride membrane 15 nm thick. (b) The frequency of blockades observed with this pore as a function of membrane voltage illustrating the frequency drop as voltage decreases below 0.5 V. The dotted line represents a fit to the data. (c) Histograms showing the distribution of dwell times observed at 500 mV (gray) and the distribution of elapsed time spanning the instant when a blockade event triggers the voltage switch from 500 to 100 mV (blue) to the return of the current to the open pore value seconds later. The peak in the distribution of current blockade durations (blue) increases from about 900 μs to about 1.5 s, increasing 1500$\times$. (d), (e) Histograms showing the distribution of the current during the blockade in the interval when λ-DNA is trapped (e), and the open pore (f). The distribution for the trapped molecule must be fitted to at least two Gaussians: one (solid blue) offset from the median ($\Delta I = 0$) by $\Delta I = +7.01$ pA with a width of $\sigma = 17.7$ pA; and another (solid red line) offset by -6.92 pA with a width of $\sigma = 18.0$ pA. The black line represents the sum. In contrast, the data in (f) representing the open pore can be fitted by a single Gaussian with a width $\sigma = 10.1$ pA.

frequency of blockade events given in figure 4(b) is about $U = 0.48 \pm 0.04$ V, which is not substantially larger than the pore of figure 1. The large blockade current estimated to be $\Delta I/I_0 = 0.65 \pm 0.11$ supports our contention that the pore diameter is smaller. In figure 4(c) we show an analysis of an extraordinary event obtained from this pore, which represents λ-DNA trapped by first applying a bias of 500 mV (near threshold) across the membrane, and then, once the onset of a blockade is detected, the voltage is switched to 100 mV (below threshold). We observe that the current returns to the open pore value near $t = 70.6$ s and the molecule exits the
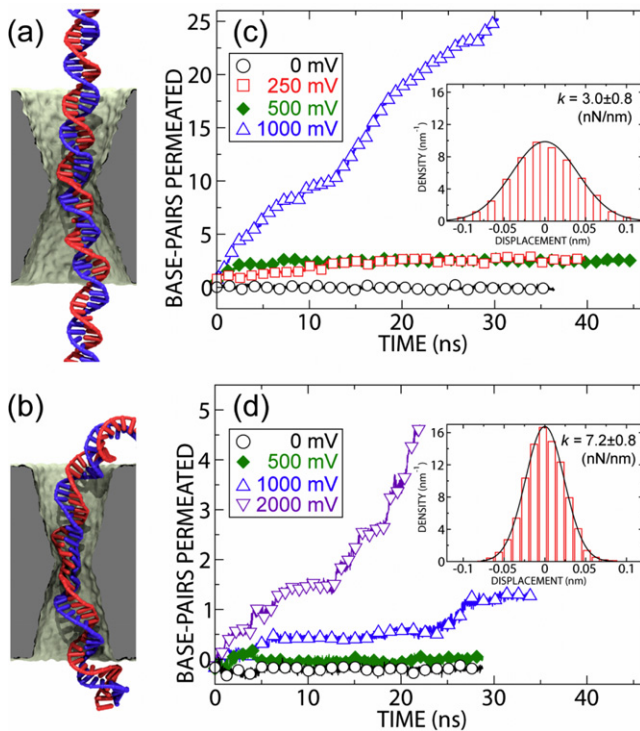
Figure 5. MD simulation of the nanopore trap. (a), (b) Snapshots of the simulated systems that include dsDNA and water and ions (not shown) as well as a 2.6 nm × 2.1 nm-cross section (a) or a 2.0 nm diameter (b) pore. The dsDNA within the constriction is stretched beyond 0.34 nm/base-pair by 0–9% (larger pore) or 20–30% (smaller pore), depending on the external bias voltage. (c), (d) The number of base-pairs permeating through the larger (c) or the smaller (d) pore in four MD simulations carried out at different biases. The simulations predict a voltage threshold between 500 mV and 1.0 V in both cases. (Insets) Normalized histogram of the DNA displacement in the pore constriction at a 0 V bias. The solid line shows the distribution expected for a particle restrained by a harmonic spring with a 3.0 nN nm^{-1} (larger pore) or a 7.2 nN nm^{-1} (smaller pore) spring constant.

pore after about 56.7 s. With the molecule trapped, we filtered the current data using a 10–600 Hz bandpass filter and formed histograms of the current fluctuations using 0.5 s windows. The trapped data shown in figure 4(c) can be represented by the two Gaussian distributions: one (solid blue) offset from the median ($\Delta I = 0$) by $\Delta I = +7.01$ pA with a width of $\sigma = 17.8$ pA; and another (solid red) offset by $\Delta I = -6.92$ pA with a width of $\sigma = 18.0$ pA. While the offsets are comparable to those observed in the 2.6 nm pore, the widths of the distributions are ~2.4× larger. The data shown in figure 4(d), which represent the open pore current data fitted by a single Gaussian with a width $\sigma = 10.1$ pA measured at the same voltage, show the same noisy trend.

After repeating the trapping experiment hundreds of times on the same pore, a comparison between the distribution of the duration of blockades observed at 500 mV, and the time that expires between the triggered voltage switch from 500 to 100 mV and the return of the current to the open pore value reveals the dichotomy illustrated in figure 4(e). This distribution is generally shifted toward an even longer time in this smaller pore in comparison with the larger pores

of figures 2(b) and 3(d), with blockades most frequently taking $t_D = 1.5$ s, as opposed to 500 or 200 ms. This suggests that the translocation velocity at the peak must have slowed substantially to a value of about (48.5 kbp–200 μs × 1 bp/19 ns)/2 s = 1 bp/53 μs, which is about 1500× slower than the velocity obtained at 500 mV.

MD simulations corroborate our interpretation of the experiments by showing that the motion of the dsDNA can be slowed or effectively stopped when the driving voltage is turned off. We created two models of nanopore systems to explore the differences between silica and silicon nitride pore surfaces that may be produced by the cleaning procedures used in the experiments, each having different pore dimensions. Figures 5(a) and (b) illustrate the simulated systems, which include fragments of dsDNA, 100 mM KCl, and a nanopore having an elliptical 2.6 nm × 2.1 nm cross-section (figure 5(a)) or a circular 2.0 nm diameter cross-section (figure 5(b)). The molecular conformation within the 2.6 nm × 2.1 nm pore was nearly unstretched at a bias of 0 V, having a length per base-pair that deviated little from its equilibrium value of 0.34 nm. In contrast, the dsDNA within the 2.0 nm pore was substantially stretched to 0.41 nm per base-pair even at 0 V. The distortion from the B-form dsDNA structure can be clearly seen in figure 5(b). Under application of a 500 mV transmembrane bias, the dsDNA was stretched to 0.37 nm/bp in the larger pore and 0.44 nm/bp in the smaller pore. As illustrated in figure 5(c), at 250 and 500 mV, the dsDNA's motion in the 2.6 nm × 2.1 nm pore was arrested following a small initial displacement allowed by stretching. Only when a bias of 1000 mV was applied was dsDNA transport observed. Likewise, transport of dsDNA in the smaller pore was only observed for biases of 1000 mV and above as shown in figure 5(d). At the same bias, the rate of dsDNA transport was much higher for the larger pore.

The insets of figures 5(c) and (d) characterize displacements of the base-pair nearest to the pore constriction in the simulations performed at a 0 V bias. The figures show normalized histograms of the displacement from the average position in the pore. The histograms have a Gaussian form, which implies that the pores act as harmonic traps for the dsDNA in the pore constriction with effective spring constants of 3.0 ± 0.8 and 7.2 ± 0.8 nN nm^{-1} for the larger and smaller pores, respectively. The probability of an escape from a trap depends sharply on the force applied to the molecule, explaining the thresholds in figures 5(c) and (d). The force required to restart the motion is essentially determined by the product of the spring constant, k, and the distance over which escape of a base-pair from the trap occurs, x_0, i.e. $q^*E \sim kx_0$. The trap profile should be invariant for displacing dsDNA by one base-pair, so $x_0 = L/2$, where L is the length per base-pair. Therefore, we estimate $kx_0 = 510$ pN for the 2.6 nm × 2.1 nm pore and $kx_0 = 1500$ pN for the 2.0 nm pore.

4. Conclusion

In summary, it is now possible to slow a single dsDNA molecule by stretching it using a nanopore, smaller in diameter

than the double helix. According to MD simulations, the dsDNA is stretched in the pore constriction with the base-pairs tilted, while the B-form canonical structure is preserved outside the pore [6, 10]. In this configuration, the translocation velocity can be substantially reduced from ~1 bp/10 ns to ~1 bp/2 ms in the extreme. We find that temporal current fluctuations associated with the molecule trapped in the pore are larger than the $1/f$ noise associated with electrolyte and, unlike the open current, it cannot be fitted to a single Gaussian. These fluctuations are tentatively attributed to the difference in current between C–G(G–C) and A–T(T–A) base-pairings in λ-DNA.

It is especially timely to consider the prospects for sequencing a DNA molecule trapped in a nanopore in this way. With the advent of next-generation-sequencing technologies, it has become exponentially harder to assemble a genome from short reads provided by extensions of conventional sequencing technology as the number of repeats grows [28]. Nanopore sequencing is advantageous above all because it has the potential for very long (>1 kbp) reads—48.5 kbp λ-DNA was measured in this study—reducing the computational burden posed by alignment and genome assembly, while at the same time eliminating logistically challenging and error-prone amplification and library formation due to its exquisite single molecule sensitivity. But the fidelity of the read is still important.

According to the protocols developed here, nanopore sequencing of dsDNA might be accomplished by simply measuring the electrolytic current that develops when a molecule, immersed in electrolyte, is forced by an electric field to translocate through a solid-state nanopore smaller in diameter than the double helix. At low bias, the nucleotides trapped in the constriction are in a tilted configuration and present a distinct energy barrier to the ions with a passage rate that is exponentially related to the height. So, the height differences for different sequences should have substantial effects on the current. One obvious problem with sequencing in this way is determining which nucleotide is on which strand, e.g. distinguishing not just C–G from T–A, but C–G from G–C. MD simulations show that the base-pair tilt caused by the confinement is maintained during a translocation with the nucleotides of one strand always lagging their partners on the other [10]. However, work presented here and elsewhere [27] indicates that it is difficult to discriminate A–T from T–A, and C–G from G–C in 100 mM electrolyte for voltages <200 mV. A substantial improvement in signal-to-noise is still required for sequencing in this way.

Acknowledgments

References

[1] Ashkin A 1997 Optical trapping and manipulation of neutral particles using lasers *Natl Acad. Sci.* **94** 4853–60

[2] Krüger P, Luo X, Klein M W, Brugger K, Haase A, Wildermuth S, Groth S, Bar-Joseph I, Folman R and Schmiedmayer J 2003 Trapping and manipulating neutral atoms with electrostatic fields *Phys. Rev. Lett.* **91** 233201

[3] Meek S A, Bethlem H L, Conrad H and Meijer G 2008 Trapping molecules on a chip in traveling potential wells *Phys. Rev. Lett.* **100** 153003

[4] Branton D *et al* 2008 The potential and challenges of nanopore sequencing *Nat. Biotechnol.* **26** 1146–53

[5] Mirsaidov U, Timp W, Zou X, Dimitrov V, Schulten K, Feinberg A P and Timp G 2009 Nanoelectromechanics of methylated DNA in a synthetic nanopore *Biophys. J.* **96** L32–43

[6] Zhao Q, Comer J, Dimitrov V, Yemenicioglu S, Aksimentiev A and Timp G 2008 Stretching and unzipping nucleic acid hairpins using a synthetic nanopore *Nucleic Acids Res.* **36** 1532–41

[7] Lederer H, May R P, Kjems J K, Baer G and Heumann H 1986 Solution structure of a short DNA fragrment studied by neutron-scattering *Eur. J. Biochem.* **161** 191–6

[8] Heng J B, Aksimentiev A, Ho C, Marks P, Grinkova Y V, Sligar S, Schulten K and Timp G 2005 Stretching DNA using the electric field in a synthetic nanopore *Nano Lett.* **5** 1883–8

[9] Heng J B, Aksimentiev A, Ho C, Marks P, Grinkova Y V, Sligar S, Schulten K and Timp G 2006 The electromechanics of DNA in a synthetic nanopore *Biophys. J.* **90** 1098–106

[10] Comer J, Dimitrov V, Zhao Q, Timp G and Aksimentiev A 2009 Microscopic mechanics of hairpin DNA translocation through synthetic nanopores *Biophys. J.* **96** 593–608

[11] Timp W, Mirsaidov U M, Wang D, Comer J, Aksimentiev O and Timp G 2010 Nanopore sequencing: electrical measurements of the code of life *IEEE Trans. Nanotechnol.* **9** 281–94

[12] Mirsaidov U M, Wang D, Timp W and Timp G 2010 Molecular diagnostics for personal medicine using a nanopore *Wires Rev. Nanomed. Nanobiotechnol.* **2** 367–81

[13] Ho C, Qiao R, Heng J B, Chatterjee A, Timp R J, Aluru N R and Timp G 2005 Electrolytic transport through a synthetic nanometer-diameter pore *Proc. Natl Acad. Sci. USA* **102** 10445–50

[14] Dimitrov V, Mirsaidov U, Wang D, Sorsch T, Mansfield W, Miner J, Klemens F, Cirelli R, Yemenicioglu S and Timp G 2010 Nanopores in solid-state membranes engineered for single molecule detection *Nanotechnology* **21** 065502

[15] Smeets R M M, Keyser U F, Dekker N H and Dekker C 2008 Noise in solid-state nanopores *Proc. Natl Acad. Sci. USA* **105** 417–21

[16] Aksimentiev A, Heng J B, Timp G and Schulten K 2004 Microscopic kinetics of DNA translocation through synthetic nanopores *Biophys. J.* **87** 2086–97

[17] Aksimentiev A 2010 Deciphering ionic current signatures of DNA transport through a nanopore *Nanoscale* **2** 468–83

[18] Cruz-Chu E R, Aksimentiev A and Schulten K 2006 Water-silica force field for simulating nanodevices *J. Phys. Chem.* B **110** 21497–508

[19] Vanbeest B W H, Kramer G J and Vansanten R A 1990 Force-fields for silicas and aluminophosphates based on *ab initio* calculations *Phys. Rev. Lett.* **64** 1955–8

[20] Vollmayr K, Kob W and Binder K 1996 Cooling-rate effects in amorphous silica: a computer-simulation study *Phys. Rev.* B **54** 15808–27

[21] Wells D B, Abramkina V and Aksimentiev A 2007 Exploring transmembrane transport through alpha-hemolysin with grid-steered molecular dynamics *J. Chem. Phys.* **127** 125101

[22] Wendel J and Goddard W 1992 The Hessian biased force field for silicon nitride ceramics: predictions of thermodynamic and mechanical properties for a- and β-Si$_3$N$_4$ *J. Chem. Phys.* **97** 5048–62

[23] Goychuk I and Hanggi P 2002 Ion channel gating: a first-passage time analysis of the Kramers type *Proc. Natl Acad. Sci. USA* **99** 3552–6

[24] Fologea D, Uplinger J, Thomas B, McNabb D S and Li J L 2005 Slowing DNA translocation in a solid-state nanopore *Nano Lett.* **5** 1734–7

[25] Storm A J, Storm C, Chen J H, Zandbergen H, Joanny J F and Dekker C 2005 Fast DNA translocation through a solid-state nanopore *Nano Lett.* **5** 1193–7

[26] Smeets R, Dekker N and Dekker C 2009 Low-frequency noise in solid-state nanopores *Nanotechnology* **20** 095501

[27] Wang D, Shim J, Timp W, Mirsaidov U, Comer J, Aksimentiev A and Timp G 2010 *Nat. Nanotechnol.* submitted

[28] Pop M and Salzberg S L 2008 Bioinformatics challenges in new sequencing technologies *Trends Genet.* **24** 142–9